The Journal of Neuroscience, February 1, 1997, 17(3):1179–1196

Spatiotemporal Patterns of Spindle Oscillations in Cortex and Thalamus

Diego Contreras,[1] Alain Destexhe,[1] Terrence J. Sejnowski,[2] and Mircea Steriade[1]

[1]Laboratoire de Neurophysiologie, Faculté de Médecine, Université Laval, Québec, Canada G1K 7P4, and [2]The Howard Hughes Medical Institute, The Salk Institute for Biological Studies, La Jolla, California 92037

Spindle oscillations (7–14 Hz) appear in the thalamus and cortex during early stages of sleep. They are generated by the combination of intrinsic properties and connectivity patterns of thalamic neurons and distributed to cortical territories by thalamocortical axons. The corticothalamic feedback is a major factor in producing coherent spatiotemporal maps of spindle oscillations in widespread thalamic territories. Here we have investigated the spatiotemporal patterns of spontaneously occurring and evoked spindles by means of multisite field potential and unit recordings in intact cortex and decorticated animals. We show that (1) spontaneous spindle oscillations are synchronized over large cortical areas during natural sleep and barbiturate anesthesia; (2) under barbiturate anesthesia, the cortical coherence is not disrupted by transection of intracortical synaptic linkages; (3) in intact cortex animals, spontaneously occurring barbiturate spindle sequences occur nearly simultaneously over widespread thalamic territories; (4) in the absence of cortex, the spontaneous spindle oscillations throughout the thalamus are less organized, but the local coherence (within 2–4 mm) is still maintained; and (5) spindling propagation is observed in intact cortex animals only when elicited by low intensity cortical stimulation, applied shortly before the initiation of a spontaneous spindle sequence; propagation velocities are between 1 and 3 mm/sec, measured in the anteroposterior axis of the thalamus; increasing the intensity of cortical stimulation triggers spindle oscillations, which start simultaneously in all leads. We propose that, *in vivo*, the coherence of spontaneous spindle oscillations in corticothalamic networks is attributable to the combined action of continuous background corticothalamic input initiating spindle sequences in several thalamic sites at the same time and divergent corticothalamic and intrathalamic connectivity.

Key words: sleep spindles; synchronization; thalamus; cortex; corticothalamic feedback; multisite recordings

Oscillatory activity in neural networks has been intensively studied over the past years. Neuronal oscillations are the basis of many different behavioral patterns and sensory mechanisms. Efforts to understand basic oscillatory mechanisms have been undertaken at the single cell level, although the rules that govern the distribution, recurrence, and coherence of oscillations over large networks have proved to be far more complex and elusive. Common principles probably underlie the spatiotemporal patterns of different oscillatory types. Spindle oscillations, consisting of waves at 7–14 Hz grouped in sequences that recur periodically, usually every 2–5 sec (Steriade and Deschênes, 1984), represent the epitome of early sleep stages and are a favorable example of oscillatory behavior in thalamocortical networks to determine those general principles, because many basic cellular mechanisms are already well understood (Steriade et al., 1990, 1993b).

Mechanisms underlying spindles have been proposed since the demonstration that this oscillation is generated within the thalamus (Morison and Bassett, 1945). An early model (Andersen and Andersson, 1968) postulated the existence of a network consisting of short-axoned inhibitory interneurons driven by intranuclear axonal collaterals of thalamocortical (TC) cells and generating IPSPs back onto TC cells that would fire rebound spike-bursts at the offset of IPSPs. In that model, the corticothalamic feedback projection played no role in the generation and distribution of spindles.

Subsequently it was shown that (1) TC cells do not give rise to intranuclear axonal recurrent collaterals (Yen and Jones, 1983; Steriade and Deschênes, 1984); (2) spindle-related IPSPs in TC cells are produced by GABAergic thalamic reticular (RE) neurons because, after disconnection from RE inputs, the IPSPs become short and arrhythmic, and spindling is abolished in dorsal thalamic nuclei (Steriade et al., 1985); and (3) the isolated rostral pole of the RE nucleus is capable of generating spindling rhythmicity (Steriade et al., 1987). During spindles, RE cells generate rhythmic (7–14 Hz) spike-bursts superimposed on a depolarizing envelope, whereas TC cells fire rebound bursts when the IPSPs imposed by RE cells are hyperpolarized enough (Steriade and Deschênes, 1988) to remove inactivation of the low threshold Ca^{2+} spike (Jahnsen and Llinás, 1984). TC spike-bursts are transferred to cortex and induce rhythmic EPSPs, which are the origin of the EEG spindle waves. In contrast with the earlier idea that corticothalamic projections play no significant role in spindling, cortical stimulation synchronizes RE neurons and enhances thalamic spindles, even by stimulating the contralateral cortex to avoid backfiring of TC axons and consequent activation of RE cells (Steriade et al., 1972; Contreras and Steriade, 1996).

Early recordings showed a high degree of spatiotemporal variability from one spindle sequence to the next, but some spindle sequences appeared nearly simultaneously in distant cortical fields (see Fig. 6.4*B* in Andersen and Andersson, 1988). Other studies, using recordings with very short interelectrode distances, showed

Received Nov. 8, 1996; accepted Nov. 25, 1996.

This work was supported by the Medical Research Council of Canada, Human Frontier Science Program, and The Howard Hughes Medical Institute. D.C. was a PhD student supported by the Savoy Foundation. We thank P. Giguère and D. Drolet for technical assistance.

Correspondence should be addressed to Professor M. Steriade at the above address.

that spindles may propagate within restricted thalamic networks (Verzeano and Negishi, 1960; Verzeano, 1972). *In vitro* studies of neurotransmitters and receptor types involved in spindling (Von Krosigk et al., 1993; Bal et al., 1995a,b) have demonstrated and quantified the propagation of spindle sequences in thalamic sagittal slices from ferret's lateral geniculate–perigeniculate region (Kim et al., 1995). Recently, we reported that, *in vivo*, the synchronization of spontaneous spindles under barbiturate anesthesia is less well organized after decortication (Contreras et al., 1996). Here we investigate the spindle synchronization in large thalamic and cortical territories by using multisite recordings of field potentials and unit discharges in intact cortex and decorticated animals. We found that spontaneous spindle sequences appear nearly simultaneously in the thalamus and neocortex; in the cortex, this was seen not only during barbiturate anesthesia but also in natural sleep of cats and humans. Spindle propagation could only be obtained by using low intensity stimulation of corticothalamic pathways. In the light of these results, we propose that the spontaneous cortical activity determines the near simultaneity of spindles throughout the thalamus.

MATERIALS AND METHODS

Preparation in acute experiments. Twenty-six adult cats (2.5–3.5 kg) were anesthetized with pentobarbital (35 mg/kg, i.p.), paralyzed with gallamine triethiodide, and artificially ventilated with control of the end-tidal CO_2 concentration at 3.2–3.5%. Heart rate was continuously monitored, and body temperature was maintained at 37–39°C. Incision points were infiltrated with lidocaine. The depth of the anesthesia was maintained by additional doses of pentobarbital to keep a stable pattern of spindle oscillations in the electroencephalogram (EEG). For cortical recordings the surface of the suprasylvian gyrus was exposed, after resection of the overlying bone and dura, and bathed in mineral oil to prevent desiccation. Thalamic recordings were performed by lowering the electrode array through the marginal gyrus or directly penetrating the thalamus after total decortication of the ipsilateral hemisphere. Hemidecortication was performed by suction after complete exposure of the left hemisphere by removing the dura.

Recording and stimulation. Gross EEG was recorded monopolarly by means of screws inserted into the bone over the pericruciate and suprasylvian areas of the contralateral hemisphere. Recording of focal EEG and electrothalamogram (EThG) was performed with (1) two arrays of eight tungsten semi-microelectrodes (tip resistances ~1 MΩ) held together in parallel, with constant interelectrode distances of either 0.4 mm or 1 mm; and (2) two concentric bipolar electrodes of lower resistance, with deinsulated tip and ring of 0.1 mm each, separated by 0.7 mm. In cortex, the bipolar electrodes were inserted with the ring placed over the pial surface. For bipolar recordings, the polarity was adjusted to match that of the cortical depth. For monopolar recordings, the indifferent electrode was placed in the neck muscles (upward deflections indicate positivity). Signals were recorded on an eight-channel tape with bandpass of 0–9 kHz and digitized at 250 Hz or 10 kHz for off-line computer analysis of waves and spikes, respectively. Filtering of the data was performed digitally.

Stimulation of the cortex and thalamus was performed by using concentric bipolar electrodes, similar to those used for recordings (see above). For cortical stimulation, two bipolar electrodes (15 mm apart) were placed *de visu* in the most anterior and posterior parts of the suprasylvian gyrus. For thalamic stimulation, a bipolar electrode was placed stereotaxically in the lateroposterior (LP) nucleus.

At the end of the experiments the cats were given lethal doses of pentobarbital.

Chronic experiments. These were performed on four naturally sleeping cats. The technique for electrode implantation and recording has been described in detail elsewhere (Steriade et al., 1996). Spindles were also analyzed at the EEG level in three normal human subjects between 25 and 45 years old, on full night (8 hr) sleep in the laboratory, after two previous sleep sessions for habituation. Data were collected during sleep stage 2, from periods containing 15 spindle sequences, for a total of 30–60 sec. For each subject, six different epochs containing 15 spindle sequences, separated by 2–4 min, were chosen. In total, 270 spindle sequences were analyzed and essentially gave the same results, namely, frequencies between 11 and 15 Hz and cross-correlation central peaks between 0.6 and 0.9.

RESULTS

The results are presented as follows. First, we reveal the distribution of spontaneous spindles over the cortex during natural sleep and under barbiturate anesthesia, and we show data indicating that the synchronization of cortical spindles is *not* attributable to intracortical synaptic linkages. Next, we present results demonstrating the widespread synchronization of spontaneous spindles within the thalamus as well as among the thalamus and cortex in intact brain animals, and we compare this full synchronization with the less organized spatiotemporal patterns of thalamic spindles after ipsilateral decortication. Last, we show that, unlike spontaneously occurring spindles, waves within the same frequency range (7–14 Hz) propagate if elicited by low intensity stimuli applied to cortex.

Synchronization of spontaneous cortical spindles in naturally sleeping humans and cats

The distribution of sleep spindles was revealed in the averaged cross-correlations between different foci recorded simultaneously over the cortex of humans and cats (Fig. 1).

The human EEG was analyzed during sleep stage 2 ($n = 3$) from scalp locations indicated in the schematic in Figure 1 (*arrowheads*). The three waxing and waning sequences depicted in Figure 1 had spindle waves with frequencies of 12–14 Hz and recurred every 2–3 sec. Cross-correlations between the top trace (*C3A2*) and each of the other traces were calculated for 15 consecutive spindle sequences. The averaged cross-correlations (*CROSS*) were precisely superimposed and show a frequency near 14 Hz, with central peak values of 0.6–0.9.

EEG recordings from the suprasylvian gyrus of chronically implanted naturally sleeping cats ($n = 4$) also revealed a high degree of spindling synchrony. In Figure 1 (*CAT*), EEG was recorded from the depth (~1 mm) of the suprasylvian cortex by means of six tungsten electrodes separated by 1 mm (see the scheme at *right*). Spindles occurred every 2–3 sec, and the waves had frequencies of 12–14 Hz. As for the human EEG, correlations between electrode 1 (Cx1) and each of the others were calculated from 15 consecutive spindle sequences. The averaged cross-correlations are displayed superimposed and show central peak values of up to 0.85 for a frequency of 13 Hz. Similar results were obtained from the marginal gyrus (data not shown).

Synchronization of spontaneous cortical spindles is not attributable to intracortical synaptic linkages

To manipulate the cortical and thalamic networks involved in spindling generation and distribution, we obtained the remainder of the results from cats anesthetized with pentobarbital. Barbiturate anesthesia reproduced faithfully the spindle oscillation observed in natural sleep (Fig. 2, *top panel*, before cut). EEG was recorded by means of eight tungsten electrodes separated by 1 mm and positioned in the depth of the suprasylvian gyrus (see scheme at the *bottom* of Fig. 2; electrode positions 1–8 are indicated by *black dots*). Under barbiturate anesthesia, spindle waves had a lower frequency than during natural sleep (~7 Hz), spindle sequences recurred every 1.5 to 7 sec, and they were synchronized among the eight leads (see below).

To show that the intracortical synchrony of spindling was not attributable to the abundant intracortical synaptic connections that run horizontally in the long axis of the suprasylvian gyrus (Avendaño et al., 1988; Amzica and Steriade, 1995b), we mea-

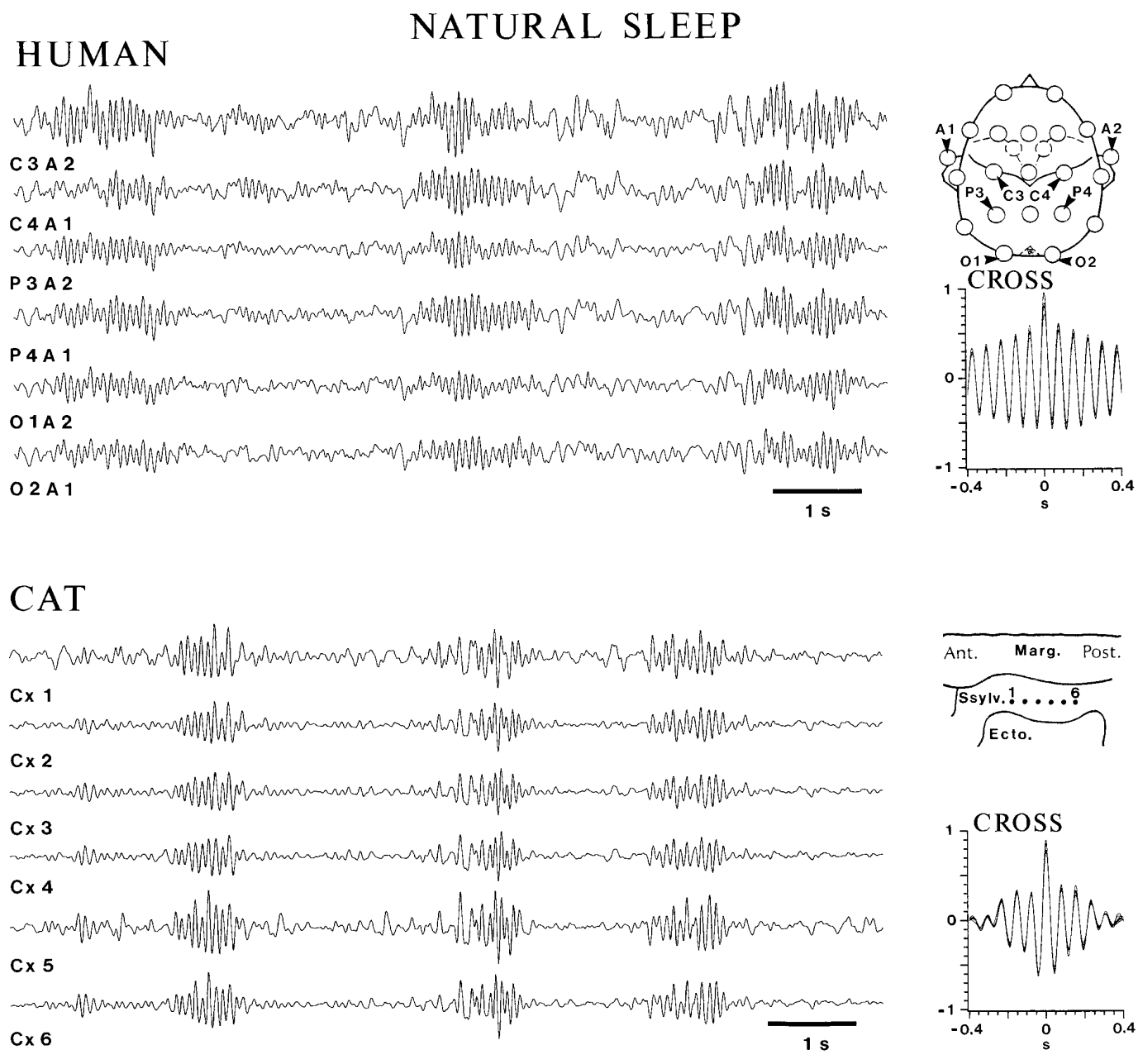

Figure 1. Cortical spindles are coherent oscillations during natural sleep. In the *top panel* (*HUMAN*), spindles were recorded from six standard EEG derivations (indicated in the schematic at *right*, *arrowheads*) in a normal subject during sleep stage 2. Cross-correlations of individual spindle sequences ($n = 15$) were calculated between C3A2 and each one of the other channels. Averaged correlations (*CROSS*) showed rhythmicity at 14 Hz and central peak values between 0.7 and 0.9. *Bottom panel* (*CAT*) shows EEG from a chronically implanted naturally sleeping animal. EEG was recorded from six tungsten electrodes separated by 1 mm, inserted in the depth of the suprasylvian gyrus (*Ssylv*), represented by *dots 1–6* in the scheme at *right*; also in the scheme are represented the ectosylvian (*Ecto.*) and the marginal (*Marg.*) gyri [anterior (*Ant.*) and posterior (*Post.*) are indicated]. The same procedure as for the human EEG was used to obtain the averaged cross-correlations depicted at *right* (*CROSS*), showing correlation at 14 Hz with central peaks between 0.75 and 0.9.

sured correlations during spindling before and after a deep coronal cut between electrodes 4 and 5 (Fig. 2, *After cut*; *vertical line* on the scheme; see also the histology of the cut). Before the cut, the averaged cross-correlations between individual spindle sequences from electrode 1 and the other cortical leads showed a progressive decrease in the value of the central peak from 0.9 to 0.4 ($n = 15$; Fig. 2, *CROSS*, *Before cut*). The coronal cut severed the tissue around electrodes 4 and 5, and the signal from that area became almost zero, thus giving rise to flat cross-correlograms 1–4 and 1–5 ($n = 15$; Fig. 2, *CROSS*, *After cut*). Nonetheless, spindling in the other electrodes continued to occur normally, and the values of the central peaks in the mean correlation between electrode 1 and the others still showed a progressive decrease from 0.9 (between leads 1 and 2) to 0.5 (between leads 1 and 8).

Widespread synchronization of spontaneous spindles in the thalamus of intact cortex hemisphere

To study the synchrony between cortical and thalamic spindles, we lowered an array of eight tungsten electrodes into the thalamus and placed two bipolar electrodes (15 mm apart) in the anterior

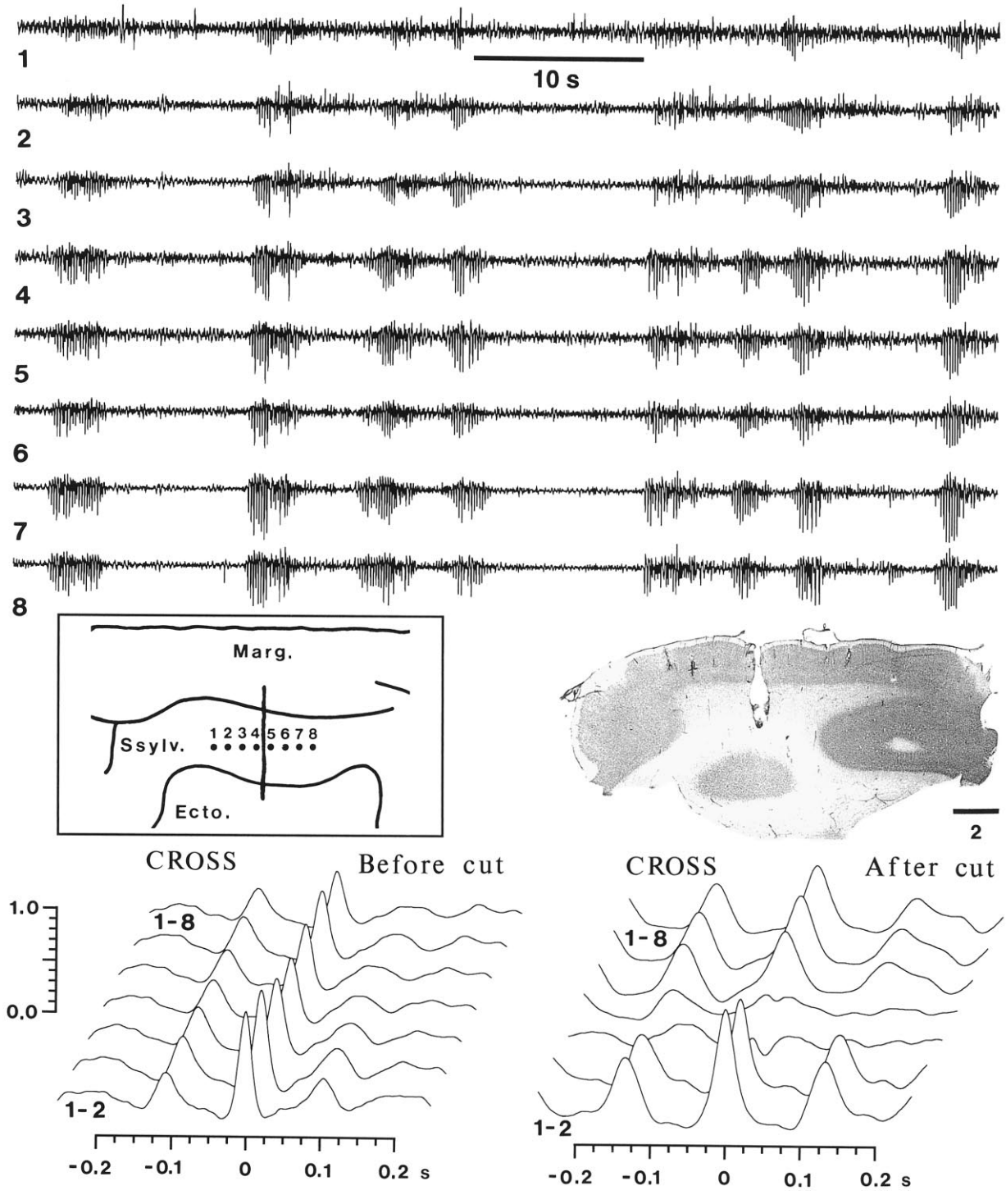

Figure 2. Cortical coherence of spindling under barbiturate anesthesia does not depend on intracortical horizontal connections. Spontaneous spindle oscillations were recorded from the depth (~1 mm) of the suprasylvian cortex by means of eight tungsten electrodes (scheme, *dots* numbered *1–8*) with interelectrode distances of 1 mm. Spindling sequences in the raw data (*top panel*, cortical leads *1–8*) showed frequencies at 7–9 Hz, lasted 2–5 sec, and recurred every 2–7 sec almost simultaneously in all electrodes. Cross-correlations between electrode *1* and each of the others, for consecutive individual spindles ($n = 15$), were averaged (*below*; *CROSS*, *Before cut*; traces were displaced horizontally and vertically for clarity) and showed central peak values decreasing from 0.9 (*1–2*) to 0.5 (*1–8*). *After cut* shows averaged cross-correlations ($n = 15$) calculated after a deep cut between electrodes *4* and *5* (*black line* on the scheme) that crossed from the marginal gyrus (*Marg.*) to the ectosylvian gyrus (*Ecto.*). The histology of the cut is shown (*right* to the scheme of recording electrodes) in a parasagittal section along the suprasylvian gyrus (anterior at *left*; calibration bar in mm); some tracks of recording electrodes are also seen. After the transection, cross-correlations showed a similar decrease in central peak from 0.9 (*1–2*) to 0.5 (*1–8*). Correlations *1–4* and *1–5* were flat because of the local lesion produced by the cut.

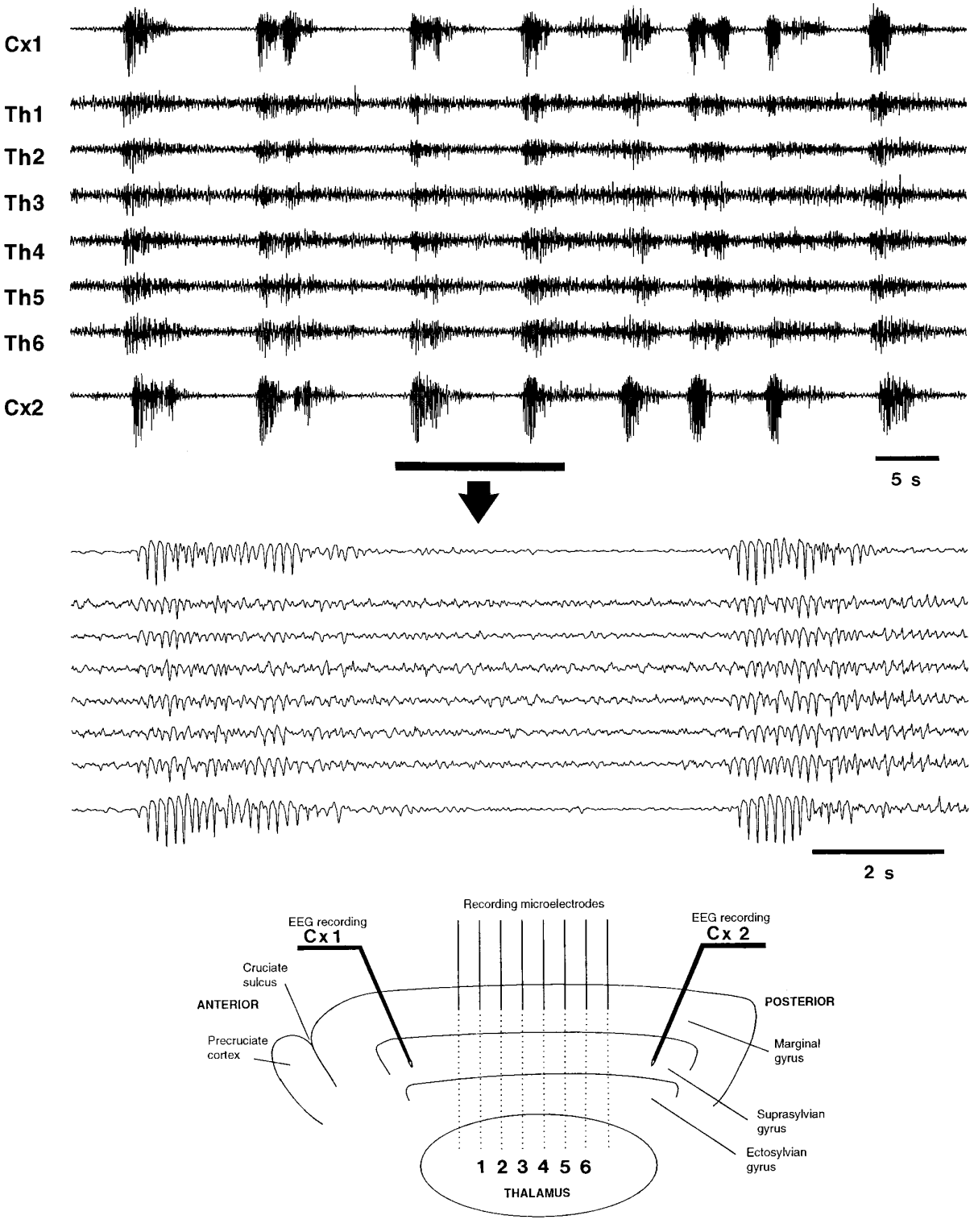

Figure 3. Spindles are synchronized between the cortex and the thalamus. *Top panel* shows spontaneous spindle sequences under barbiturate anesthesia, recorded by two bipolar electrodes located in the depth of the suprasylvian gyrus and separated by 15 mm (*Cx1* and *Cx2*) and by six tungsten electrodes in the anteroposterior axis of the thalamus (*Th1–Th6*). The arrangement of recording electrodes is depicted in the schematic *below*; the thalamic electrodes penetrated through the marginal gyrus (*dotted lines*). A detail of two spontaneous spindle sequences, indicated by *bar*, is expanded *below* (*arrow*). Note that spindles occurred nearly simultaneously in all leads.

and posterior parts of the suprasylvian gyrus (Fig. 3, see scheme at *bottom*). The near simultaneity of thalamic and cortical spindles is demonstrated in the two expanded spindle sequences (*arrow*).

The widespread simultaneity of spindling in the thalamus was shown by recording from an array of eight tungsten electrodes separated by 1 mm and positioned in the anteroposterior axis of the thalamus at various stereotaxic planes. The thalamus was explored with the 8-electrode array, from anterior planes 13 to 6,

from lateral planes 2 to 5, and from depths +4 to +1, with a total of 52 penetrations in 26 investigated animals. No more than two descents per animal were allowed to avoid tissue damage. Penetrations associated with absence of spindling in several leads and bleeding in the thalamus and/or cortex were not analyzed. The example depicted in Figure 4 is representative of the most common result, which was independent of the position on the thalamic map ($n = 38$). It was occasionally possible to detect the presence of local spindles, occurring in only one or a few electrodes (Fig. 4, *top, arrows*). The coincidence in time of spindle initiation and termination, recorded from the eight thalamic electrodes, was shown by calculating the sequential power spectrum ($n = 16$) from contiguous windows of 0.5 sec in each channel. The total power between 7–14 Hz from each window was then plotted against time (Fig. 4, *bottom*). Because absolute values of power had no significance, they were normalized so that the highest peak was 1. The presence of synchronous spindles was revealed qualitatively by the simultaneous increase and decrease of the values of total power in the eight channels. The strong intrathalamic synchrony of spindling was shown by averaging the cross-correlations of consecutive spindle sequences ($n = 15$) between electrode 1 and the other electrodes (Fig. 4, *Averaged CROSS*; the first trace is the autocorrelation from electrode 1). The value of the central peaks of the averaged cross-correlations decreased from 0.83 between electrode 1 and 2 to 0.54 between 1 and 8 (Fig. 4, *Peak CROSS*).

The temporal coincidence, across thalamic electrodes, of the spindling local field potentials (LFPs) presumably reflects near-simultaneity of spindle sequences in groups of neurons. Multiunit recordings from RE and TC cells (Fig. 5) were obtained by using tungsten microelectrodes inserted with the same spatial configurations as for LFPs. Spindle-related spike-bursts were grouped in spontaneous sequences occurring in close time relation among different electrodes (Fig. 5, *panel 1*; the position of most anterior electrode is indicated). The first spindle sequence (indicated by *horizontal bar* marked *2*) is expanded at right (Fig. 5, *panel 2*) and shows that individual cells fired spike-bursts at irregular frequencies, but the population frequency was consistently 7–8 Hz across one spindle sequence (see also Fig. 2*A* in Steriade et al., 1977). To study the time dispersion of individual spindle sequences at different electrode sites, we calculated average rates from the multiunit spikes and took the first burst in each spindle sequence from TC1 as time reference. The average rates from the other electrodes were aligned to the time marks selected from TC1. The dispersion in time of the rate was larger for cells located more distantly from the reference TC1; in other words, spindle-related burst firing occurred within narrower time windows for closer, than for distant, cells (compare TC1 and TC2, separated by 1 mm, with TC7 and TC8, distant from TC1 by 6 and 7 mm, respectively). This pattern of increased dispersion in spindle-related cellular activity with increased distance was obtained independently of which cell was chosen as reference and is in agreement with the decrease in synchrony with distance in spindling LFPs (see Fig. 4, *bottom*).

Besides generalized spindling, spindle sequences could be confined to one or two thalamic foci. In the example of Figure 6, thalamic cell populations and their corresponding field potentials were recorded simultaneously from eight sites separated by 1 mm in the anteroposterior axis (TC1–TC8). Average rates were calculated from the multiunit spikes. The first two spindle sequences occurred at similar times in all eight electrodes, as seen in the LFPs and rate meters. Local spindling occurred in TC7 and TC8 after the second spindle sequence and prevented the occurrence of the next spontaneous spindle in those leads (*arrows*). The next delayed spindle sequence seemed to be initiated near TC7 and TC8.

Alterations in thalamic synchronization of spontaneous spindles after decortication

The most likely candidate for the global coherence of spindle sequences in the thalamus is the massive corticothalamic feedback projection (see introductory remarks). To test this possibility, we performed complete decortications of one hemisphere ($n = 18$). As shown in the example of Figure 7, the neocortex was completely removed. Only structures medial to the rhinal sulcus (prepiriform and periamygdaloid cortices) were left intact, but they are not implicated in spindling.

Recordings of thalamic LFPs, ipsilateral to the decortication, often lacked coordinated spontaneous spindle sequences across the thalamus (Fig. 8; see *detail 1* below). In other instances, however, spindles occurred almost simultaneously throughout the thalamus (Fig. 8; *detail 2*), suggesting that there is an intrathalamic mechanism for global synchronization. Twenty percent of spindle sequences ($n = 126$) in decorticated animals were nearly simultaneous, and such highly synchronous spindles alternated with disorganized ones (Fig. 8). In comparison with the intact cortex condition, the sequential power spectrum of traces from different electrodes, calculated in contiguous windows of 0.5 sec, and the total power between 7–14 Hz displayed against time after normalization (Fig. 8, *bottom panel*) no longer had their values increasing and decreasing in a concerted manner. Global thalamic synchrony was still observed on occasions (*asterisk* in power spectrum corresponding to the *asterisk* in the *top panel*; see also other synchronized spindle sequences in the *right* part of the *top panel* with LFPs).

A likely candidate for the preserved global coherence of thalamic spindles in the absence of cortex is the RE nucleus. Indeed, whereas there is virtually no crosstalk among TC cells and spindles are abolished in the dorsal thalamus after disconnection from the RE nucleus (Steriade et al., 1985), the rostral part of the RE nucleus projects to many dorsal thalamic nuclei and generates spindle rhythmicity even after disconnection from thalamic and cortical afferents (Steriade et al., 1987). We hypothesized that the divergent projections from the rostral pole and rostrolateral sector of the RE nuclear complex to more posterior sites in the dorsal thalamus (see Fig. 10 in Steriade et al., 1984) would be implicated in the global coherence of thalamic spindles after decortication. In support of this possibility, we found that, in some instances, spindle sequences are initiated earlier in rostral RE cells, as compared with TC cells recorded more posteriorly (Fig. 9). When both cellular types were recorded simultaneously in decorticated animals ($n = 6$), propagation patterns were observed in three cases, with spike-bursts from RE cells preceding those from TC neurons by one or two cycles. In such instances propagation velocities varied from 1.5 to 3 mm/sec. In the example of Figure 9, channel 1 depicts RE cells, as demonstrated by prolonged bursting with a characteristic accelerando–decelerando firing pattern (see detail indicated by *asterisk* below). The first spindle sequence, indicated by a horizontal bar, is expanded below (*arrow*). The first spike-bursts of RE cells preceded the first bursts of TC1 cells by 240 msec, and similar times separated the bursts of other TC cells, thus giving an approximate propagation velocity of 1.6 mm/sec. Precedence of TC cells by the bursting of RE cells could also be seen in the average of the rates from 15 consecutive spindle sequences depicted in the right column of Figure 9 from

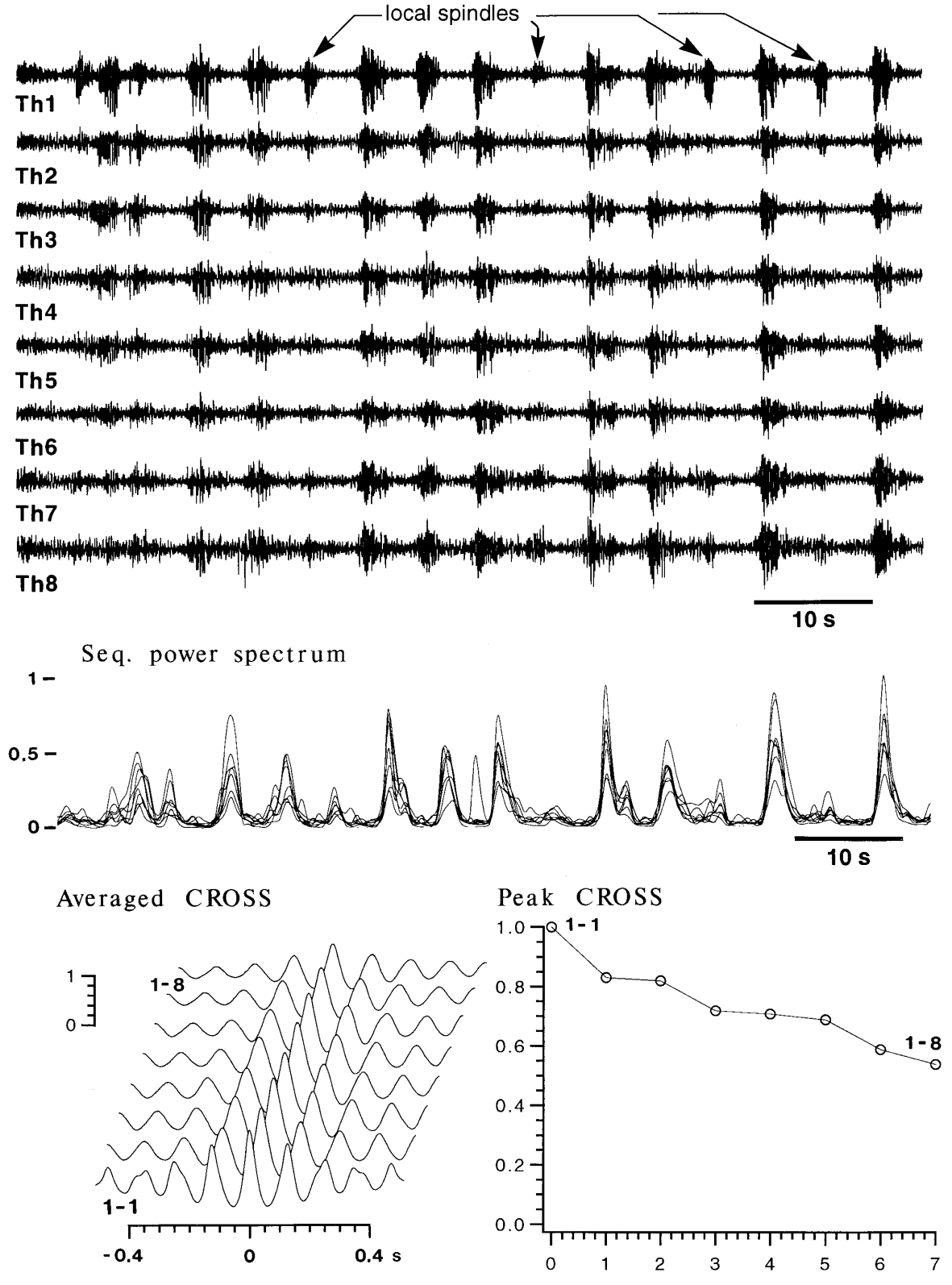

Figure 4. Coherent spindle oscillations over large thalamic territories. Spontaneous spindling was recorded under barbiturate anesthesia from eight thalamic areas (*Th1–Th8*) separated by 1 mm in the anteroposterior axis of the thalamus, from anterior planes 13 to 6 (3 mm lateral from the midline, depth +3). Spindles were simultaneous in all leads except for shorter spindle sequences that occurred almost exclusively in most rostral electrode 1 (*local spindles*). *Below*, *Seq. power spectrum* was calculated for each channel from contiguous windows of 0.5 sec. Total power between 7–14 Hz from each window was normalized to the highest value in each channel and displayed against time. The values of power increased and decreased together in all channels. Cross-correlations were computed between individual spindle sequences ($n = 15$) from channel 1 and the others and averaged (*Averaged CROSS*; *1–1* is the autocorrelogram of channel 1). The value of the central peak of the seven averaged cross-correlations is plotted at *right* (*Peak CROSS*) and shows a decrease from 0.8 to 0.6.

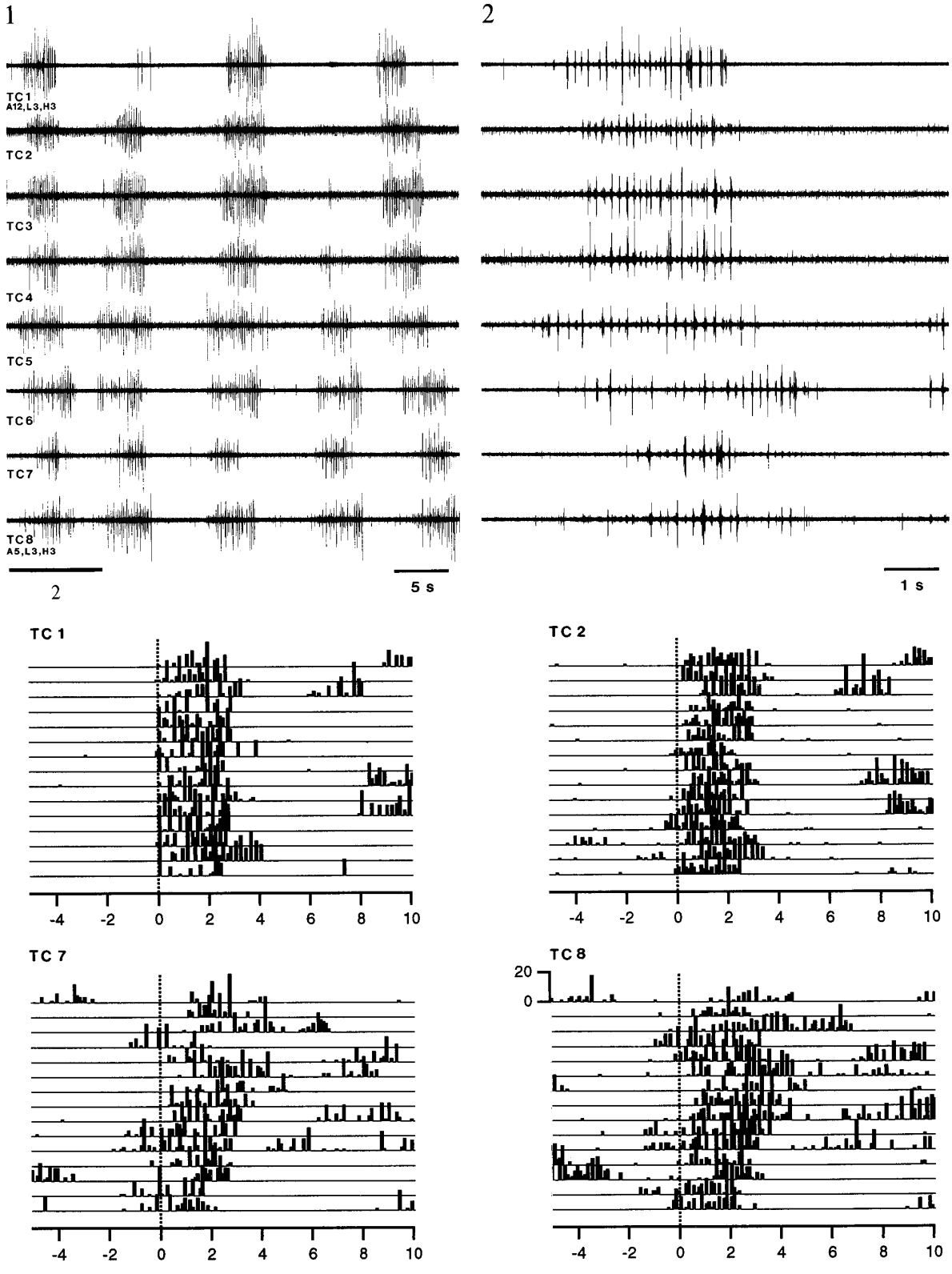

Figure 5. Thalamic cells discharge spike-bursts grouped in spindle sequences in close time relation throughout the thalamus. Multiunit recordings from TC cells were simultaneously obtained from eight tungsten microelectrodes (*TC1–TC8*), separated by 1 mm in the anteroposterior axis of the thalamus (position of most anterior electrode is indicated). Spontaneous spindling activity is shown in *1*. Spindle sequence indicated by *horizontal bar* is expanded at *right*, in *2*. Average rates were computed for each channel (bin size, 0.1 sec), and time of first burst in *TC1* was used as marker for aligning the other traces. Fifteen consecutive spindle sequences are shown *below* for four channels (*TC1*, *TC2*, *TC7*, and *TC8*; abscissa scale is in seconds). *Dotted line* indicates time of the first burst from *TC1* in each spindle sequence. Time dispersion of burst firing increased with the distance to the reference cell.

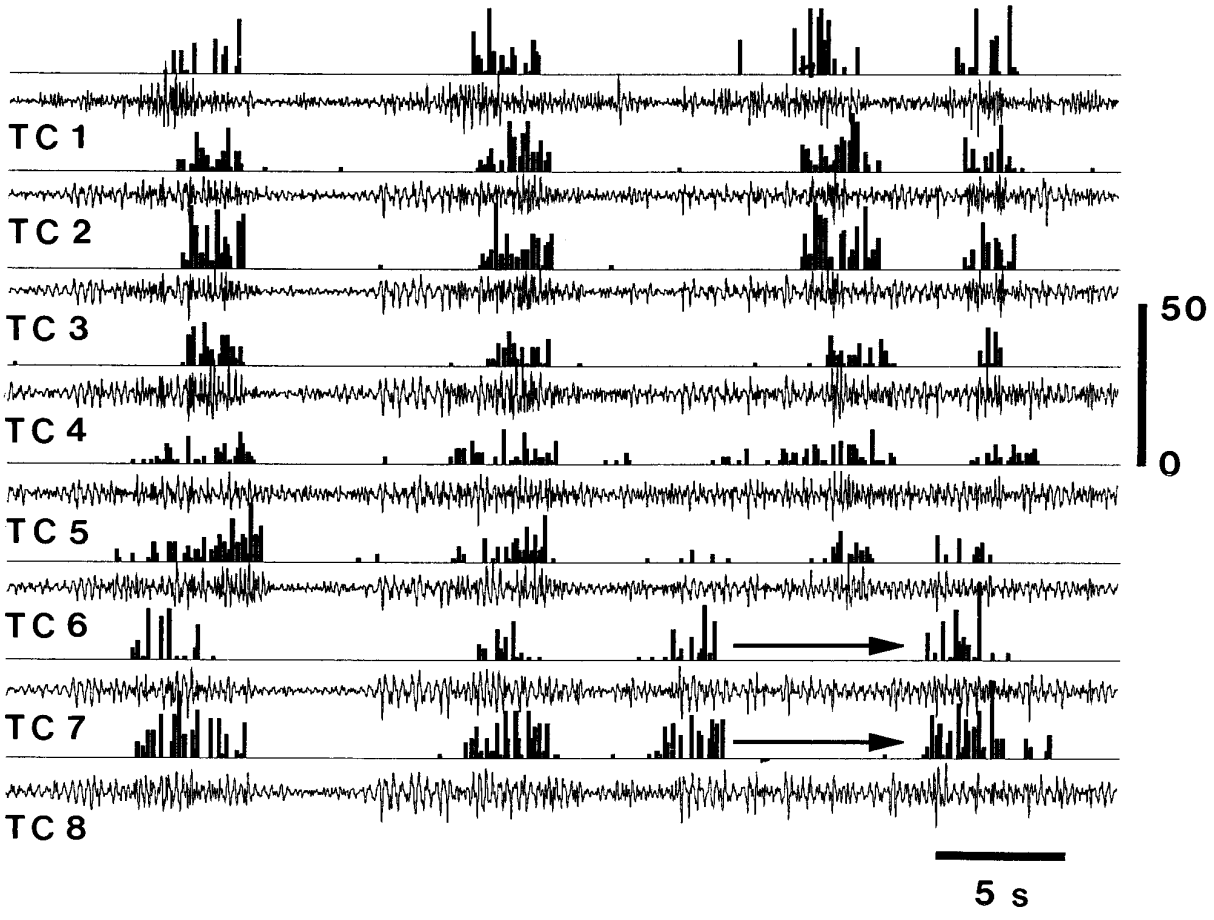

Figure 6. Local spindling prevents participation in global spindling. Multiunit recordings and LFPs were obtained from eight thalamic sites. Average rates were calculated (bin size, 0.1 sec) and depicted with the corresponding LFP for each channel (*TC1–TC8*). The two first spontaneous spindle sequences occurred simultaneously in LFPs from all electrodes. Local spindling in *TC7* and *TC8* prevented next global spindling to reach those electrodes (*arrows*).

RE, TC4, and TC6 cells. The first burst of the RE cell in each spindling sequence was taken as time reference and rate meter activity from TC cells aligned to it. Ensemble averaging the rates from each channel showed that RE firing consistently preceded TC firing (*bottom panel*). We have to mention, however, that, with random sampling of RE and TC cells, it is more likely to see spindles in RE cells first, because they fire in higher percentages of cycles within each spindle wave.

Propagation of spindles evoked by low intensity cortical and thalamic stimulation

Propagation of spindling in the absence of the cortex could be attributable to the pattern of divergent connections between RE and TC cells. Spindling may thus be initiated in a single focus and propagate away from the site of initiation. To trigger a spindle sequence in a confined area of the thalamus artificially, we used low intensity cortical stimulation.

Spindle sequences were consistently evoked by cortical stimulation. In the example of Figure 10, EEG was recorded from the depth of the suprasylvian gyrus (~1 mm) with an array of eight electrodes (Cx1–Cx8, anterior to posterior, 1 mm interelectrode distance). Bipolar stimulating electrodes were positioned 3–4 mm anteriorly and posteriorly to the electrode array (see similar arrangement in the scheme in Fig. 3 showing cortical recording electrodes). High intensity stimulation applied through the posterior stimulating electrode elicited an early response that decreased in amplitude with distance from Cx8 to Cx1 (*top panel*; early response is expanded at *right*, and stimulation is represented by *dotted line*) and was followed by a spindle sequence occurring synchronously in all eight electrodes (*top panel, left*). By decreasing the intensity down to 15% of maximal stimulation, we were able to initiate a spindle sequence that traveled away from the stimulating electrode (*second panel, left*), in which case the initial response barely reached more anterior electrodes (*second panel, right*). A mirror image was obtained with anterior suprasylvian stimulation (*bottom panel*).

It should be mentioned that low intensity stimulation only triggered propagating spindles when applied shortly *before* (0.1–0.4 sec) an expected spontaneously occurring spindle sequence, i.e., at the end of an interspindle period. In the earlier part of the interspindle lull, an evoked potential was produced by the low intensity stimulation that was not followed by a spindle sequence. The period between spontaneous spindle sequences (2–10 sec) varied among animals; within the same experiment it depended on the depth of the anesthesia. The threshold for evoking a spindle sequence with low intensity stimulation also varied. Therefore, timing and intensity of stimulation had to be adjusted for each series of stimuli. Time of stimulation was adjusted by measuring the interspindle period from five consecutive spontaneous spindle sequences; intensity was then adjusted empirically to find threshold intensity, which varied between 10 and 30% of maximal

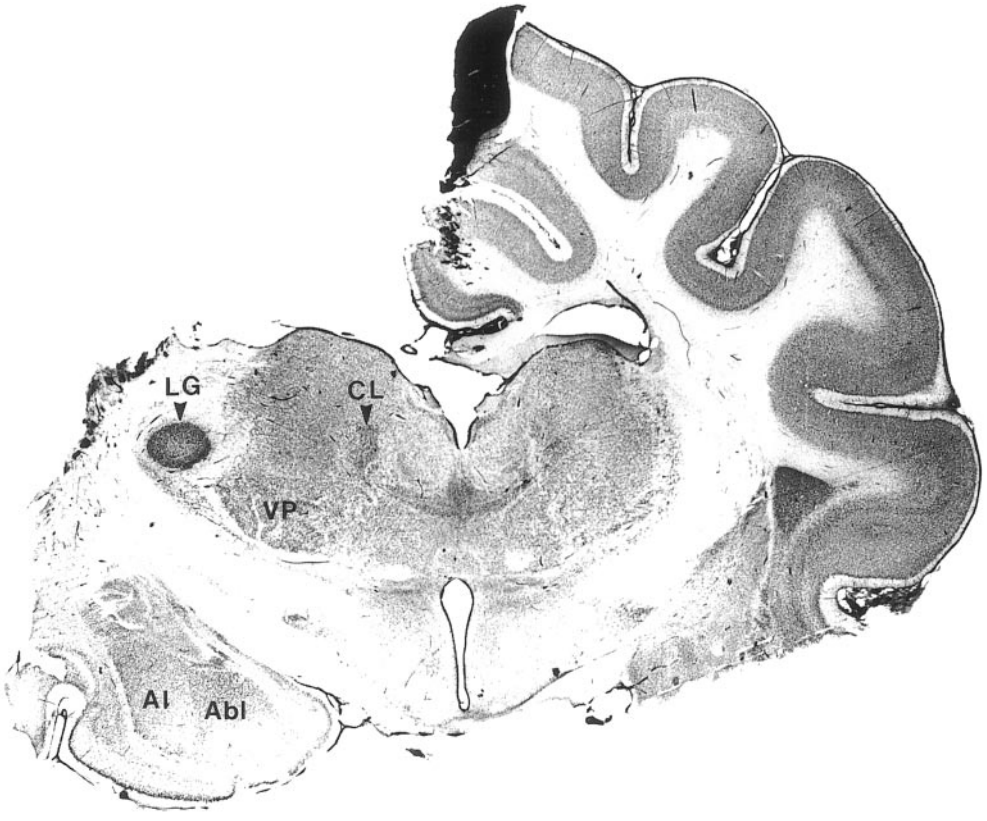

Figure 7. Decortication of left hemisphere. Nissl-stained coronal section showing hemidecortication and cut of the corpus callosum. The *black spot* on the medial wall of the right hemisphere is attributable to crystals of $AgNO_3$ used against bleeding during decortication. *Al, Abl*, Lateral and basolateral nuclei of amygdala; *CL*, centrolateral intralaminar nucleus; *LG*, lateral geniculate nucleus; *VP*, ventroposterior complex.

intensity. In contrast, high intensity stimulation was capable of eliciting synchronized spindle sequences shortly after the termination of a spontaneous spindle sequence.

To rule out the possibility that the propagation of spindle sequences was attributable to intracortical horizontal connections, we performed a deep coronal cut (similar to that depicted in Fig. 2) between electrodes Cx4 and Cx5 and applied stimulation at both extremes of the suprasylvian gyrus (Fig. 11; $n = 6$). After the cut, the intensity of stimulation had to be increased, probably because of the tissue damage. The effect of the cut was visible in traces from electrodes 4 and 5, which became almost flat because of local lesion; the early evoked potential was also strongly diminished, up to disappearance, on the other side of electrodes 4 and 5 (see details at *right*). No effect, however, was visible in the propagation pattern of evoked spindles.

To test the hypothesis that the propagation of spindle sequences in the cortex reflects orderly propagation in the anteroposterior axis of the thalamus, we recorded evoked spindles in the thalamus with an array of eight electrodes (TC1–TC8, 1 mm interelectrode distance) while applying a cortical stimulation paradigm ($n = 8$) similar to that used above to obtain cortical propagation. Indeed, low intensity stimuli to anterior suprasylvian cortex triggered a spindle sequence of spike-bursts in the most anterior thalamic electrode (TC1) that traveled away from that electrode (Fig. 12*, 1*, *arrow*). Propagation in the opposite direction was obtained by low intensity stimulation to the posterior suprasylvian cortex (Fig. 12*, 2*). As in the case of cortically recorded spindles, propagation was only obtained when stimulation was applied shortly before the initiation of an expected spontaneous spindle sequence. The synchronizing power of the corticothalamic projection became evident by increasing the intensity of stimuli applied to the anterior or the posterior suprasylvian sites: in each case a spindle sequence was obtained that occurred coherently over the whole thalamic area being recorded (data not shown).

To assess the reliability of the propagation of spindle sequences in the thalamus on cortical stimulation, we measured average rates from the cell populations TC1–TC8 and calculated the ensemble average of the rates from 15 consecutive evoked spindle sequences (Fig. 13). Propagation was obtained consistently in the posterior-to-anterior direction by posterior cortical stimulation (*top panel*), and the reverse was obtained by anterior cortical stimulation (*middle panel*). By increasing the intensity of stimulation applied to the anterior site (*bottom panel*) or posterior site (not shown) of suprasylvian gyrus, we observed that propagation no longer occurred; instead, spindles started almost simultaneously in all thalamic sites.

DISCUSSION

We have reported three major findings. (1) In intact brain preparations, spontaneous spindles are nearly simultaneous over large thalamic and neocortical territories. (2) In decorticated animals, the spatiotemporal patterns of spontaneous spindles are less coherent, although the local thalamic synchronization (2–4 mm) is preserved, and even global synchrony is occasionally observed throughout the thalamus. (3) In the intact cortex animal, propagating spindles are consistently observed only when evoked by low intensity stimulation of corticothalamic projections, whereas increasing the strength of cortical volleys leads to simultaneity of spindles throughout the thalamus and cortex.

Although most experimental procedures have been performed in animals under barbiturate anesthesia and spindles have been recorded from the suprasylvian gyrus, similar results showing the near-simultaneity of spontaneous spindle sequences have been obtained in this study by recordings from the marginal gyrus and

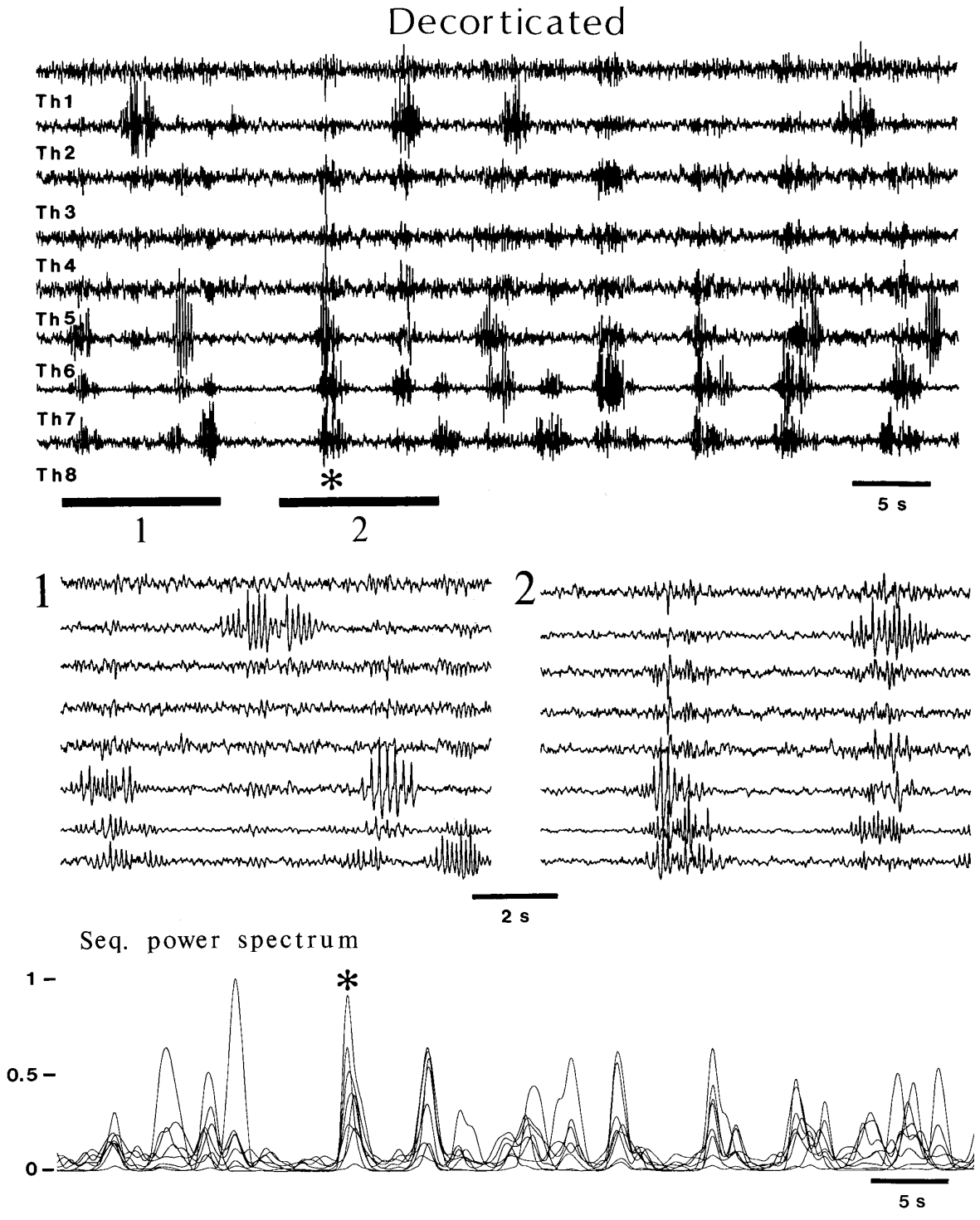

Figure 8. Strong spatiotemporal coherence of thalamic spindle oscillations is lost after ipsilateral decortication. Eight thalamic foci (*Th1–Th8*), corresponding to the electrodes indicated in the scheme of Figure 7, were recorded simultaneously after complete ipsilateral decortication. Parts indicated by *bars 1* and *2*, expanded *below*, show examples of lack of temporal coordination between spindle sequences (in *1*) but also epochs with well organized, simultaneous spindle sequences in many different thalamic foci (in *2*; see also such coherent spindle sequences in the *right* part of the *top panel*). At *bottom*, *Seq. power spectrum* was calculated as in Figure 4. Overall, changes in total power were no longer simultaneous among different thalamic channels. However, *asterisks* (in the *top panel* with LFPs, as well as in power spectrum, showing the same spindle sequence) indicate one of the spindle sequences that were synchronized throughout the thalamus.

by using multisite cortical recordings from the suprasylvian gyrus during natural sleep stage 2. We have also observed nearly simultaneous spindle sequences during natural sleep of cat by recording the activity from motor, visual, and suprasylvian cortices as well as appropriate thalamic nuclei (F. Amzica, D. Neckelmann, M. Steriade, unpublished data). Because spindles are generated in the thalamus and we have also shown that cortical synchrony is not attributable to intracortical projections, data collected during

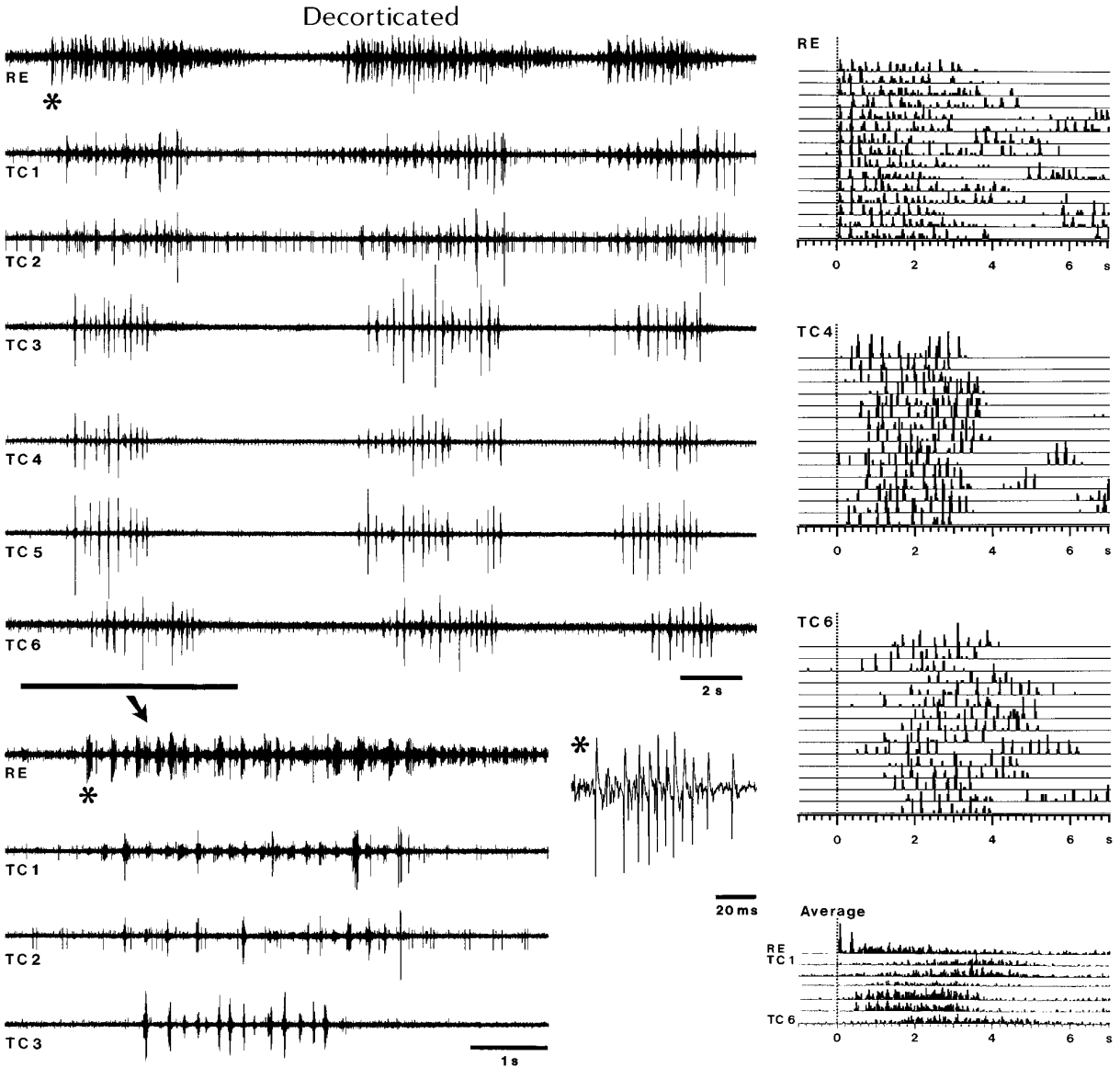

Figure 9. Spike-bursts from rostral RE cells may precede those from TC cells during spontaneous spindling after decortication. Multiunit recordings from the RE nucleus and six thalamic foci (*TC1–TC6*) were recorded simultaneously with 0.4 mm interelectrode distances. Spike-bursts from three spontaneous spindles are shown in which firing of RE cells consistently preceded TC firing. The first spindle sequence (*bar*) is expanded *below* (*arrow*). Average rates were computed (bin size, 0.1 sec), and first burst from RE cells at each spindle sequence was taken as time 0 to align the rate meters from the other cells. (*Right column* depicts *RE*, *TC4*, and *TC6*. *Average* includes rates from RE and all TC cells.) Fifteen consecutive spindle sequences show that spike-bursts from RE cells preceded those from TC cells. A tendency for increased delay with distance suggested that thalamic propagation may occur in decorticated conditions.

natural sleep suggest that a widespread synchrony of spindle sequences occurs in the thalamus of unanesthetized animals and humans.

Simultaneity of spontaneous spindle sequences in the intact brain

At variance with the results from *in vitro* experiments in the visual thalamus indicating clear-cut propagation of spindle sequences with a definite direction in sagittal slices (Kim et al., 1995), our *in vivo* experiments showed absence of propagation of spontaneous spindles. First, we propose two mechanisms that may account for the highly coherent patterns of spontaneous spindle sequences observed in our *in vivo* experiments. Next, we advance two explanations for the major difference between *in vivo* and *in vitro* results.

First, in the *in vivo* condition, under anesthesia and even more so in unanesthetized animals, spindle sequences are generated at the same time at many different thalamic foci because of the high background activity in corticothalamic networks. The slow rhythm of thalamic spindle sequences (generally 0.2–0.5 Hz) has a frequency similar to that of the cortical slow oscillation (Steriade et al., 1993c). The cortical origin of the slow oscillation was demonstrated by its survival in cortex of athalamic animals (Steriade et al., 1993d) and its absence in the thalamus of decorticated animals (Timofeev and Steriade, 1996). Antidromically identified corticothalamic neurons display slow oscillations, followed by spindles (see Fig. 5*C,D* in Steriade et al., 1993d). The spindle sequences are ascribed to the cortical-elicited synaptic activation of thalamic neurons within the frequency range of the slow oscillation (Ste-

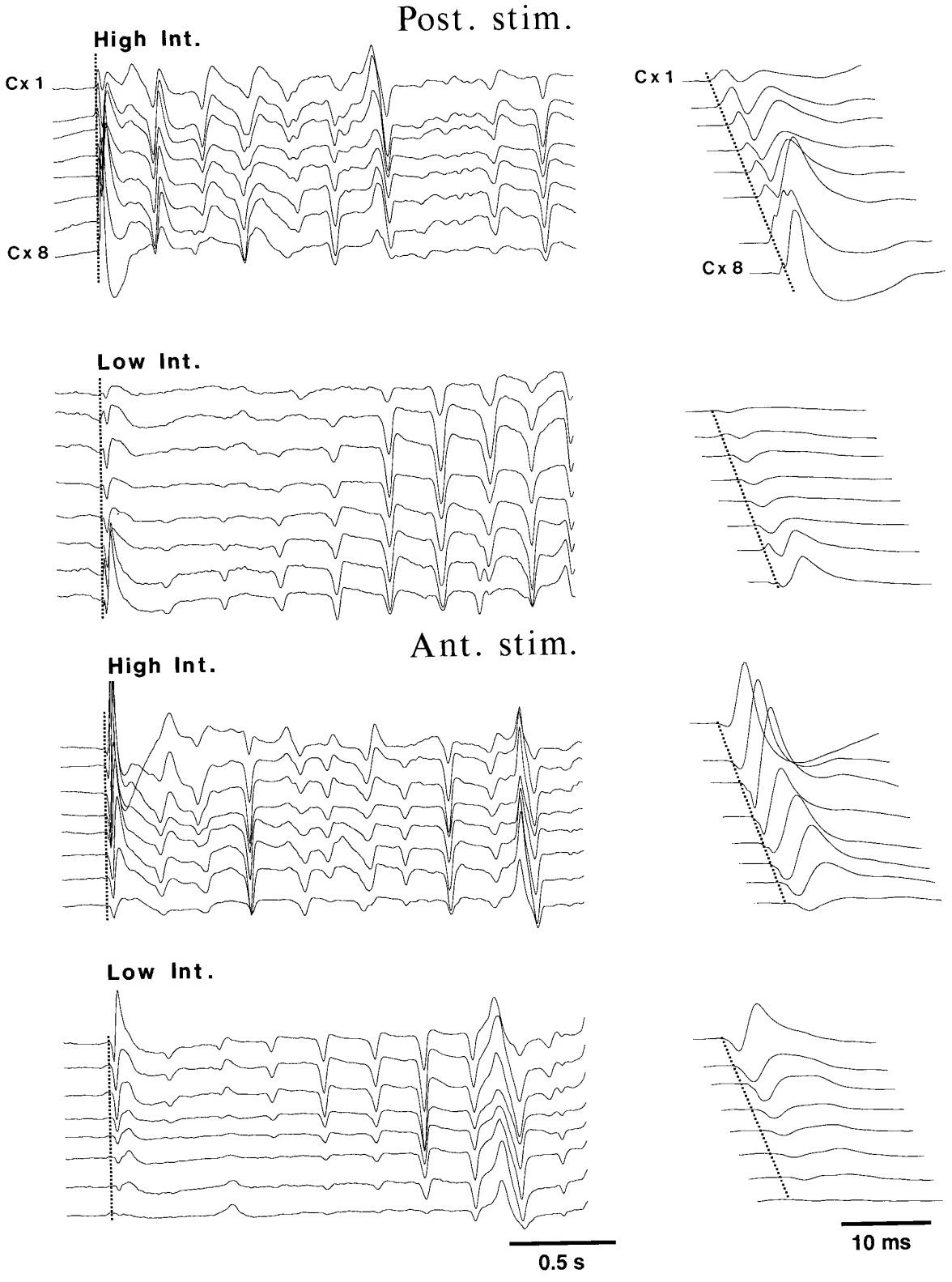

Figure 10. Cortical stimulation with low intensity triggers spindle sequences that travel away from the stimulating site. LFPs were recorded from eight tungsten electrodes (*Cx1–Cx8*) inserted in the depth (~1 mm) of the suprasylvian cortex. Stimuli were applied through bipolar electrodes situated 4 mm in front and 4 mm behind the electrode array (see similar location of recording cortical electrodes in the scheme of Fig. 2 and similar location of stimulating cortical electrodes in the schematic with cortical recording electrodes of Fig. 3). Synchronized spindling was triggered by high intensity stimulation in the posterior part of the suprasylvian gyrus (*top panel*; initial response expanded at *right*, with sweeps displaced horizontally). Low intensity stimulation at the same posterior site triggered spindling that propagated to more anterior foci (*second panel*; initial response, expanded at *right*, barely reached electrode *Cx1*). Anterior stimulation also gave rise to full synchrony of evoked spindles on high intensity volleys (*third panel*), whereas propagation was from anterior to posterior sites by using low intensity stimuli (*bottom panel*).

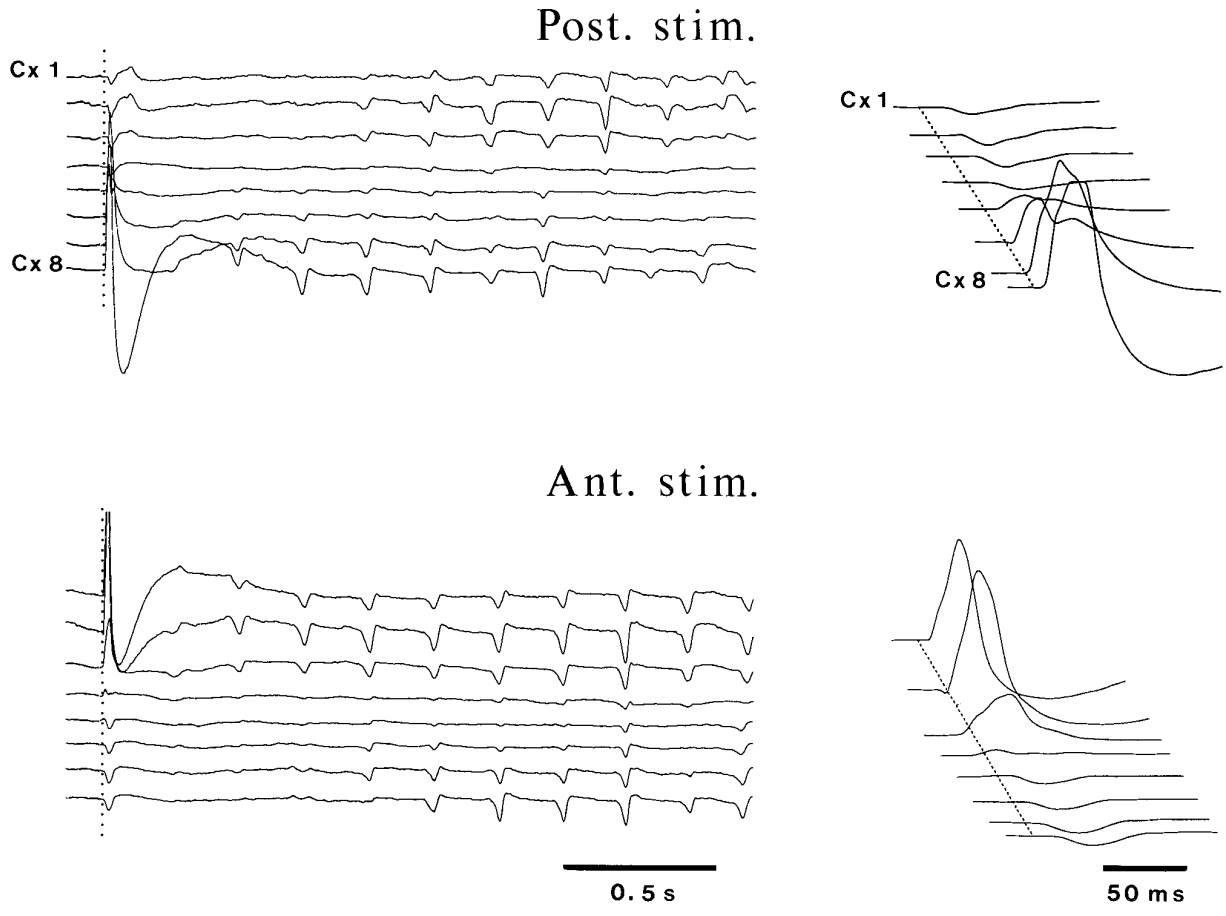

Figure 11. Intracortical horizontal connections are not implicated in spindling propagation. Same experimental conditions as in Figure 10. A deep coronal cut was performed between electrodes 4 and 5, which caused an important decrease in amplitude in those leads. Propagating spindle sequences were still observed in both directions (posterior-to-anterior and anterior-to-posterior).

riade et al., 1993a; Contreras and Steriade, 1995). Because the slow oscillation is synchronized over large neocortical territories (Amzica and Steriade, 1995a,b), we propose that many slowly oscillating cortical neuronal pools with thalamic projections would trigger RE cells nearly simultaneously, leading to coherent spindling activity in TC networks. It should be emphasized that the degree of synchronization of the cortical-generated slow oscillation is far higher than that of spindles (Contreras and Steriade, 1997) and that cortical volleys are effective in triggering synchronized spindles in the thalamus (see introductory remarks). The decisive role of the slow oscillation in pacing thalamic spindles and determining their patterns is also demonstrated under ketamine–xylazine anesthesia by the fact that (1) in the intact cortex hemisphere, thalamic spindles display a waning pattern, with almost no waxing process, because the powerful corticothalamic drive associated with the depolarizing component of the slow oscillation generates maximum synchrony of RE and TC cells from the beginning of spindle sequences (Contreras and Steriade, 1996); by contrast, (2) in the decorticated hemisphere, the presence of a waxing pattern increases the total duration of spindles five to six times compared with the simultaneously recorded intact cortex hemisphere (Timofeev and Steriade, 1996).

The second mechanism that is involved in the wide range synchronization of spindles results from the divergent connectivity in corticothalamic networks. Spindles may be initiated in single or multiple thalamic sites as a consequence of hyperpolarization–rebound sequences produced by the removal, at sleep onset, of brainstem ascending activating influences (Steriade and McCarley, 1990). However, such initially isolated oscillations would rapidly entrain the rest of the network because of the pattern of divergent connections in thalamocorticothalamic loops (Jones, 1985). In the thalamus, different cells may fire rebound spike-bursts at variable times, but they would eventually be brought to discharge synchronously by virtue of corticothalamic and intrathalamic (RE–TC) connectivity. Thus, although a certain degree of jitter may be observed in the time of spindle initiation, no consistent propagation would be observable at the large scale of the thalamus, although propagation within very small scales might occur at the beginning of each spindle sequence. The present experiments did not resolve short range propagation that has been described by using closely located, 0.03–0.1 mm, electrodes (Verzeano and Negishi, 1960). In that study, however, local propagation did not show a preferential direction, as demonstrated in thalamic slices (Kim et al., 1995), but it changed continuously in a three-dimensional pattern.

From the above, it follows that there are two major differences between the *in vivo* and *in vitro* conditions.

First, the reduced background synaptic activity in slices allows different initiator areas enough time to permit appreciable propagation. In addition, the low spontaneous activity *in vitro* and, hence, the higher input resistance renders cells more electrotonically compact and easier to be entrained into population oscilla-

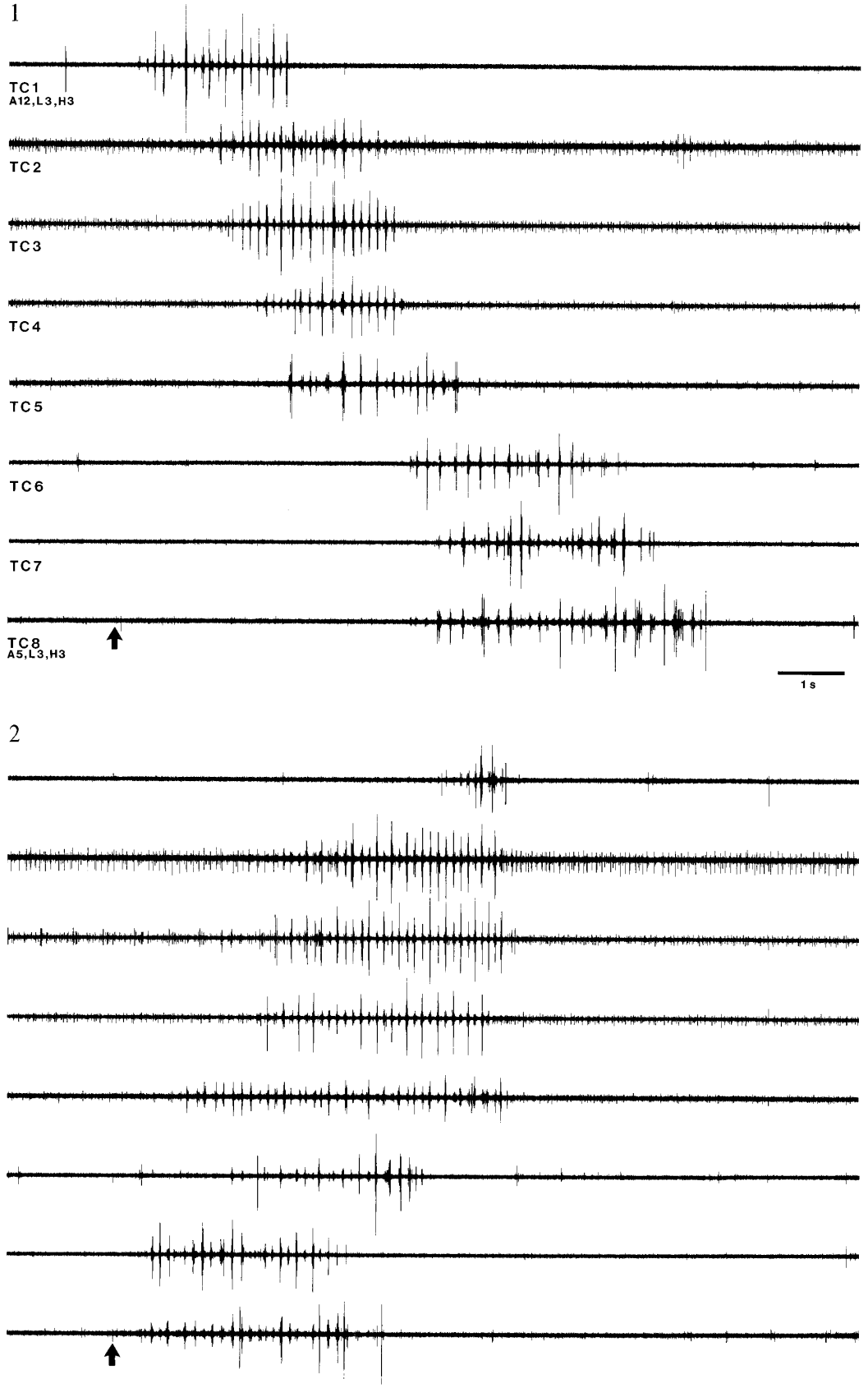

Figure 12. Evoked spindle sequences display propagation in the thalamus when low intensity stimulation is applied to cortex. Multiunit recordings of TC cells were obtained from eight locations (*TC1–TC8*) separated by 1 mm in the anteroposterior axis of the thalamus (position of the most anterior electrode is indicated). Cortical stimulation is marked by an *arrow*. *1*, Low intensity stimulation in the anterior suprasylvian gyrus generated a spindle sequence that propagated from anterior to posterior at a velocity of 1.5 mm/sec. *2*, Posterior cortical stimulation at low intensity generated a mirror image response.

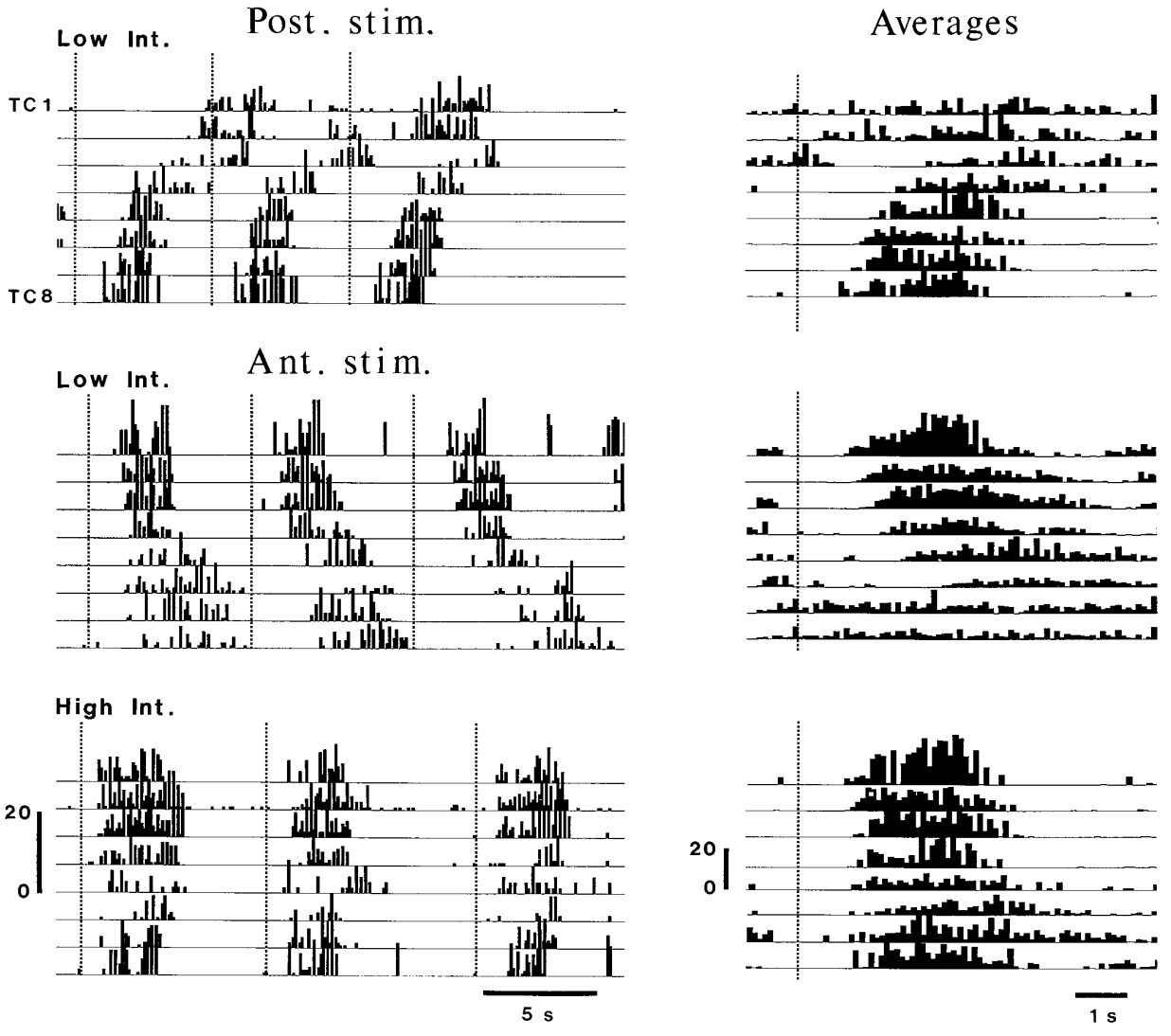

Figure 13. Cortical stimulation synchronizes spindling oscillations throughout the thalamus. Multiunit recordings were obtained from the same positions as in Figure 12, and the average rates (bin size, 0.1 sec) were calculated. *Left column* depicts examples from three consecutive stimuli. *Right column* shows averaged peristimulus histograms calculated from the rate meter data ($n = 15$). Low intensity cortical stimuli generated propagating spindle sequences when applied through the posterior (*top panel*, stimuli represented by *dotted lines*) or anterior (*second panel*) electrodes. Increasing the intensity of cortical stimulation triggered simultaneous spindle sequences in the eight thalamic electrodes.

tion, as shown by the fact that a single spike-burst from an RE cell can entrain propagating spindle sequences (Kim et al., 1995). The prediction follows that depressing the spontaneous activity of the network should reduce the global coherence of spindles and would progressively increase the dispersion time of spindle initiation. Indeed, the decrease in the central peak of the cross-correlations during cortical spindling is more pronounced under barbiturate anesthesia than in natural sleep (Fig. 1) because of the hyperpolarizing action of barbiturate on thalamic and cortical neurons, thus reducing their spontaneous discharges. In the extreme condition of spreading depression (Leao, 1944), there is an increased jitter and decreased spatial correlation of spontaneous cortical spindles (Contreras et al., 1997; A. Destexhe, D. Contreras, M. Steriade, unpublished data).

The second difference between the present *in vivo* study and the *in vitro* study by Kim et al. (1995) may be that different thalamic sectors were studied. The latter authors investigated the visual thalamus in ferret. Although the extensive overlap of dendrites of RE cells makes it unlikely that sensory maps are very accurate in the RE nuclear complex, some investigators have reported slab-like organization of TC–RE and cortico–RE projections, with rather precise topographical arrangements, in the visual (Montero et al., 1977; Crabtree and Killackey, 1989), auditory (Conley et al., 1991), and somatosensory (Shosaku et al., 1984; Pinault et al., 1995) systems (for review, see Mitrofanis and Guillery, 1993). Even in these cases, however, some RE neurons projecting to the ventroposterior (VP) nuclei were also found to ramify in the posterior (Po) thalamic group (Yen et al., 1985; Pinault et al., 1995). In contrast to these generally well organized TC–RE–TC projections in primary sensory thalamic sectors, the projection of RE neurons to thalamic association nuclei, such as the pulvinar–lateroposterior (Pul–LP) complex, are only roughly organized in a topographic manner (FitzGibbon et al., 1995). Importantly, the rostral pole and rostrolateral sector of the RE nucleus project to a variety of dorsal thalamic nuclei, among them anterior (centrolateral–paracentral, CL–PC) and posterior intralaminar nuclei,

ventroanterior–ventrolateral (VA–VL) nuclei, ventromedial (VM) and LP nuclei (Steriade et al., 1984). These data, emphasizing the more diffuse projections of the rostral part of RE nucleus, mainly directed to intralaminar CL–PC nuclei, have recently been supported by double-labeling experiments showing that the RE projections to the intralaminar and midline thalamic nuclei are far more diffuse than the RE projections to specific dorsal thalamic nuclei (Kolmac and Mitrofanis, 1997). This difference between the discrete and topographically organized connectivity linking RE and TC cells in thalamic sensory sectors and the more diffuse connectivity patterns linking RE and intralaminar nuclei may well explain the propagated spindles within the well defined circuitry of the visual thalamus (Kim et al., 1995), as opposed to the profuse cortical distribution of spindling in cortical areas afferented by thalamic nuclei with diffuse neocortical projections (Morison and Dempsey, 1942), such as CL–PC and VM. Almost simultaneous spindle oscillations in the intralaminar CL nucleus and projection neocortical areas have been described in previous studies (see Fig. 7 in Steriade et al., 1993d). The projections from the rostral RE sectors to the more caudal dorsal thalamic nuclei may account for some propagation phenomena (see Fig. 9).

Propagation of spindling by low intensity cortical stimulation

Spindle oscillations triggered by low intensity cortical stimulation propagated away from the stimulated site. The ordered propagation was reflected in both thalamic and cortical recordings, possibly because of the pattern of connectivity between large areas of the thalamus and the suprasylvian cortex (Olson and Lawler, 1987; Avendaño et al., 1990). Two variables determined the propagation of cortical-elicited spindles: the intensity of stimulation (below 5–20% of maximal strength) and the timing of stimulation with respect to the preceding spindle sequence. The fact that the threshold for evoking a spindle sequence decreased toward the end of the interspindle period suggests that a refractory period follows spindling generation *in vivo*, similar to data reported in thalamic slices (Kim et al., 1995). It has been proposed that refractoriness of spindles results from the shift in voltage dependence of the hyperpolarization-activated cation current, I_h (Destexhe et al., 1996; Bal and McCormick, 1996). Alternatively, it has been shown *in vivo* that a period of slight hyperpolarization and decreased input resistance follows spontaneous spindle sequences (Nuñez et al., 1992). However, this does not imply an absolute refractory period of the network, because it was possible to evoke spindles at any time, even during an ongoing spontaneous spindle sequence, by using strong stimuli to the cortex or white matter. This suggests that not all cells participate at each spindle sequence.

Concluding remarks

We propose that the large scale coherence of spindling *in vivo* is attributable to the combined action of two factors: (1) the background corticothalamic activity triggers burst firing in many thalamic foci during the narrow time window of lower threshold at the end of the interspindle lull; and (2) the divergent connections between cortex and thalamus, as well as between the rostral part of RE nucleus and the dorsal thalamus, assure a fast entrainment of thalamic and cortical populations into the oscillation. Data suggest that spindles arise at similar times in distant areas of the thalamus, but their generating networks (RE and TC) do not necessarily interact directly; instead, a third party, the neocortex, may intervene to achieve simultaneity of spindling among distant sites. Because of the relative absence of spontaneous activity *in vitro*, different initiator areas are separated by enough time to allow appreciable propagation. Thus, low intensity cortical stimulation *in vivo* imitates the *in vitro* condition by artificially generating a circumscribed initiator zone that precedes all other thalamic areas.

REFERENCES

Amzica F, Steriade M (1995a) Short- and long-range neuronal synchronization of the slow (<1 Hz) cortical oscillation. J Neurophysiol 73:20–39.

Amzica F, Steriade M (1995b) Disconnection of intracortical synaptic linkages disrupts synchronization of a slow oscillation. J Neurosci 15:4658–4677.

Andersen P, Andersson SA (1968) Physiological basis of alpha rhythm. New York: Appleton-Century-Crofts.

Avendaño C, Rausell E, Perez-Aguilar D, Isorna S (1988) Organization of the association cortical afferent connections of area 5: a retrograde tracer study in the cat. J Comp Neurol 278:1–33.

Avendaño C, Stepniewska I, Rausell E, Reinoso-Suarez F (1990) Segregation and heterogeneity of thalamic cell populations projecting to superficial layers of posterior parietal cortex: a retrograde tracer study in cat and monkey. Neuroscience 39:547–559.

Bal T, McCormick DA (1996) What stops synchronized thalamocortical oscillations? Neuron 17:297–308.

Bal T, von Krosigk M, McCormick DA (1995a) Synaptic and membrane mechanisms underlying synchronized oscillations in the ferret lateral geniculate nucleus *in vitro*. J Physiol (Lond) 483:641–663.

Bal T, von Krosigk M, McCormick DA (1995b) Role of the ferret perigeniculate nucleus in the generation of synchronized oscillations *in vitro*. J Physiol (Lond) 482:665–685.

Conley M, Kupersmith AC, Diamond IT (1991) The organization of projections from subdivisions of the auditory cortex and thalamus to the auditory sector of the thalamic reticular nucleus in galago. Eur J Neurosci 3:1089–1103.

Contreras D, Steriade M (1995) Cellular basis of EEG slow rhythms: a study of dynamic corticothalamic relationships. J Neurosci 15:604–622.

Contreras D, Steriade M (1996) Spindle oscillations in cats: the role of corticothalamic feedback in a thalamically generated rhythm. J Physiol (Lond) 490:159–180.

Contreras D, Steriade M (1997) Synchronization of low-frequency rhythms in corticothalamic networks. Neuroscience 76:11–24.

Contreras D, Destexhe A, Sejnowski TJ, Steriade M (1996) Control of spatiotemporal coherence of a thalamic oscillation by corticothalamic feedback. Science 274:771–774.

Contreras D, Destexhe A, Steriade M (1997) Spindle oscillations during cortical spreading depression in naturally sleeping cats. Neuroscience, in press.

Crabtree JW, Killackey HP (1989) The topographic organization and axis of projection within the visual sector of the rabbit's thalamic reticular nucleus. Eur J Neurosci 1:94–109.

Destexhe A, Bal T, McCormick DA, Sejnowski TJ (1996) Ionic mechanisms underlying synchronized oscillations and propagating waves in a model of ferret thalamic slices. J Neurophysiol 76:2049–2070.

FitzGibbon T, Tevah LV, Sefton AJ (1995) Connections between the reticular nucleus of the thalamus and pulvinar-lateralis posterior complex: a WGA-HRP study. J Comp Neurol 363:489–504.

Jahnsen H, Llinás R (1984) Ionic basis for the electroresponsiveness and oscillatory properties of guinea-pig thalamic neurones *in vitro*. J Physiol (Lond) 349:227–247.

Jones EG (1985) The thalamus. New York: Plenum.

Kim U, Bal T, McCormick DA (1995) Spindle waves are propagating synchronized oscillations in the ferret LGN *in vitro*. J Neurophysiol 74:1301–1323.

Kolmac CI, Mitrofanis J (1997) Organization of the reticular thalamic projection to the intralaminar and midline nuclei in rats. J Comp Neurol, in press.

Leao AAP (1944) Spreading depression of activity in the cerebral cortex. J Neurophysiol 7:359–390.

Mitrofanis J, Guillery RW (1993) New views of the thalamic reticular nucleus in the adult and developing brain. Trends Neurosci 16:240–245.

Montero VM, Guillery RW, Woolsey CN (1977) Retinotopic organiza-

tion within the thalamic reticular nucleus demonstrated by a double label autoradiographic technique. Brain Res 138:407–421.
Morison RS, Bassett DL (1945) Electrical activity of the thalamus and basal ganglia in decorticate cats. J Neurophysiol 8:309–314.
Morison RS, Dempsey EW (1942) A study of thalamocortical relations. Am J Physiol 135:281–292.
Nuñez A, Curró Dossi R, Contreras D, Steriade M (1992) Intracellular evidence for incompatibility between spindle and delta oscillations in thalamocortical neurons of cat. Neuroscience 48:75–85.
Olson CR, Lawler K (1987) Cortical and subcortical afferent connections of a posterior division of feline area 7 (area 7p). J Comp Neurol 259:13–30.
Pinault D, Bourassa J, Deschênes M (1995) The axonal arborization of single thalamic reticular neurons in the somatosensory thalamus of the rat. Eur J Neurosci 7:31–40.
Shosaku A, Kayama Y, Sumitomo ZI (1984) Somatotopic organization in the rat thalamic reticular nucleus. Brain Res 311:57–64.
Steriade M, Deschênes M (1984) The thalamus as a neuronal oscillator. Brain Res Rev 8:1–63.
Steriade M, Deschênes M (1988) Intrathalamic and brainstem-thalamic networks involved in resting and alert states. In: Cellular thalamic mechanisms (Bentivoglio M, Spreafico R, eds), pp 51–76. Amsterdam: Elsevier.
Steriade M, McCarley RW (1990) Brainstem control of wakefulness and sleep. New York: Plenum.
Steriade M, Wyzinski P, Apostol V (1972) Corticofugal projections governing rhythmic thalamic activity. In: Corticothalamic projections and sensorimotor activities (Frigyesi TL, Rinvik E, Yahr MD, eds), pp 221–272. New York: Raven.
Steriade M, Oakson G, Diallo A (1977) Reticular influences on lateralis posterior thalamic neurons. Brain Res 131:55–71.
Steriade M, Parent A, Hada J (1984) Thalamic projections of nucleus reticularis thalami of cat: a study using retrograde transport of horseradish peroxidase and double fluorescent tracers. J Comp Neurol 229:531–547.
Steriade M, Deschênes M, Domich L, Mulle C (1985) Abolition of spindle oscillations in thalamic neurons disconnected from nucleus reticularis thalami. J Neurophysiol 54:1473–1497.
Steriade M, Domich L, Oakson G, Deschênes M (1987) The deafferented reticularis thalami nucleus generates spindle rhythmicity. J Neurophysiol 57:260–273.
Steriade M, Jones EG, Llinás RR (1990) Thalamic oscillations and signaling. New York: Wiley.
Steriade M, Contreras D, Curró Dossi R, Nuñez A (1993a) The slow (<1 Hz) oscillation in reticular thalamic and thalamocortical neurons: scenario of sleep rhythm generation in interacting thalamic and neocortical networks. J Neurosci 13:3284–3299.
Steriade M, McCormick DA, Sejnowski TJ (1993b) Thalamocortical oscillations in the sleeping and aroused brain. Science 262:679–685.
Steriade M, Nuñez A, Amzica F (1993c) A novel slow (<1 Hz) oscillation of neocortical neurons *in vivo*: depolarizing and hyperpolarizing components. J Neurosci 13:3252–3265.
Steriade M, Nuñez A, Amzica F (1993d) Intracellular analysis of relations between the slow (<1 Hz) neocortical oscillation and other sleep rhythms of the electroencephalogram. J Neurosci 13:3266–3283.
Steriade M, Amzica F, Contreras D (1996) Synchronization of fast (30–40 Hz) spontaneous cortical rhythms during brain activation. J Neurosci 16:392–417.
Timofeev I, Steriade M (1996) The low-frequency rhythms in the thalamus of intact-cortex and decorticated cats. J Neurophysiol 76:4152–4168.
Verzeano M (1972) Pacemakers, synchronization, and epilepsy. In: Synchronization of EEG activity in epilepsies (Petsche H, Brazier MAB, eds), pp 154–158. New York: Springer.
Verzeano M, Negishi K (1960) Neuronal activity in cortical and thalamic networks. J Gen Physiol 43:177–195.
Von Krosigk M, Bal T, McCormick DA (1993) Cellular mechanisms of a synchronized oscillation in the thalamus. Science 261:361–364.
Yen CT, Jones EG (1983) Intracellular staining of physiologically identified neurons and axons in the somatosensory thalamus of the cat. Brain Res 280:148–154.